Proceedings of ICRC 2001: 2022 © Copernicus Gesellschaft 2001

ICRC 2001

The influence of electron temperature and magnetic field strength on cosmic ray injection in high Mach number shocks

H. Schmitz[1], **S. C. Chapman**[1], **and R. O. Dendy**[2]

[1]Space and Astrophysics Group, Department of Physics, University of Warwick, Coventry CV4 7AL, UK
[2]UKAEA Fusion, Culham Science Centre, Abingdon, Oxfordshire OX14 3DB, UK

Abstract.

Electron pre–acceleration from thermal to mildly relativistic energies in high Mach number shocks (the injection problem) is an outstanding issue in understanding synchrotron radiation from supernova remnants. At high Alfvénic Mach numbers, collisionless perpendicular shocks reflect a fraction of the upstream ions. This gives rise to two–stream instabilities which in turn can accelerate ions, see eg (M. E. Dieckmann *et al.*, Astron. Astrophys. **356**, 377 (2000)). However in astrophysical plasmas the value of β – the ratio of kinetic to magnetic pressure – is not well known. We have used a particle in cell simulation code to investigate the influence of β on the shock structure and on the electron acceleration. Previous simulations at low values of β (N. Shimada and M. Hoshino, Astrophys. J. **543**, L67 (2000)) showed that the phase space distributions of electrons and ions became highly structured: characteristic holes appear in the electron phase space and the shock dynamics exhibit reformation processes. However, we find that all these features disappear at higher β due to the high initial thermal velocity of the electrons. It follows that the electron cosmic ray injection mechanism depends strongly on β, that is, the electron temperature and magnetic field strength upstream.

1 Introduction

Observations of supernova remnant (SNR) shocks give clear evidence of the existence of strongly relativistic electrons (Koyama *et al* , 1995). It is believed that diffusive shock acceleration (eg Blandford & Ostriker (1978)) provides the mechanism for accelerating the electrons to such high energies. However this mechanism can only efficiently accelerate mildly relativistic electrons. This pre–acceleration problem still remains an open question (Levinson , 1996). For the case of perpendicular shocks Papadopoulos (1988) proposed that instabilities caused by the ions reflected off the shock and so creating the foot of the shock could cause the necessary electron acceleration. A number of hybrid simulations have been carried out (eg Cargill & Papadopoulos (1988)) to address this problem. These however assume a thermal electron distribution and can not account for nonthermal electron heating or acceleration. Recently Shimada and Hoshino (2000) simulated a high Mach number perpendicular shock with a fully kinetic code. In their simulations the ratio of kinetic to magnetic pressure β was fixed. The value of β in SNR shocks is however uncertain. It is therefore our aim in this paper to repeat the simulations of Shimada and Hoshino for two different values of β and compare the shock behaviour and the electron acceleration.

Correspondence to: H. Schmitz
(holgers@astro.warwick.ac.uk)

2 Simulation

We use a relativistic electro-magnetic particle in cell (PIC) code to simulate the structure and development of a high Mach number (approx. 10) magnetosonic shock. In PIC simulations the ions and electrons of the plasma are represented by super-particles while the electro-magnetic field is given on a grid in configuration space. The super-particles and the fields are advanced in time in a leapfrog algorithm using the Lorentz force to accelerate and move the super-particles and the Maxwell equations to advance the fields. Details of the PIC simulation technique are described eg by Hockney and Eastwood (1981). The PIC algorithm enables self-consistent simulations of plasmas that are far from equilibrium, where arbitrary distribution functions can develop.

The code we use to simulate the shock is described by Devine (1995) and has been used recently to investigate electron acceleration in the foot of SNR shocks (Dieckmann *et al.* (2000), Drury *et al.* (2001)). All field and bulk plasma quantities are a function of one configuration space coordinate (x) and time. The particles in addition have vector velocities. The simulated shock is assumed to be homogeneous in the y– and z–directions. To set up the shock we use the so called piston method, ie we inject particles (electrons and ions) on the left side of the simulation box, while the right bound-

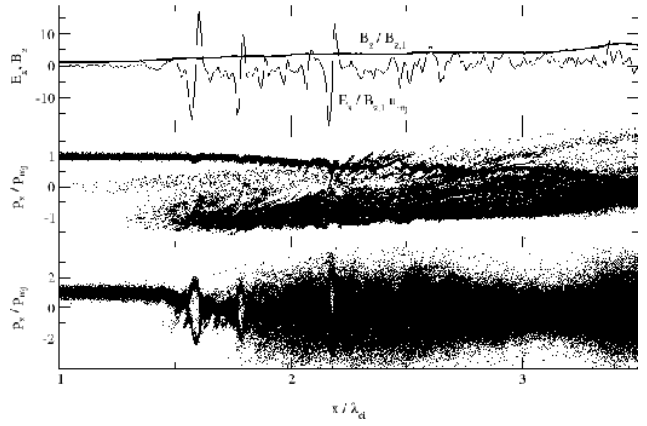

Fig. 1. The parallel electric and perpendicular magnetic field (upper panel) the ion phase space distribution (middle panel) and the electron phase space distribution (lower panel) at $t\omega_{ci} \approx 2.5$ for $\beta = 0.15$.

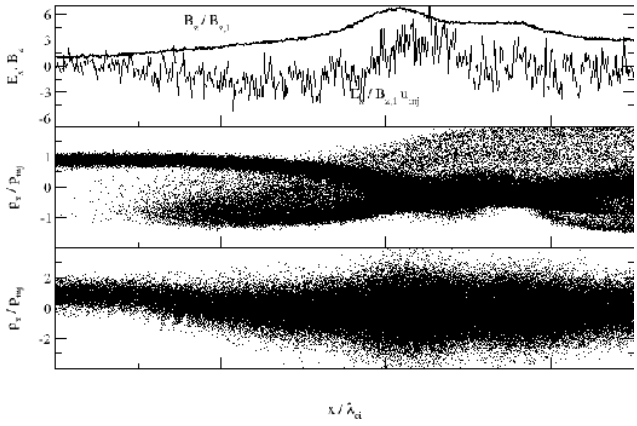

Fig. 2. The parallel electric and perpendicular magnetic field (upper panel) the ion phase space distribution (middle panel) and the electron phase space distribution (lower panel) at $t\omega_{ci} \approx 3$ for $\beta = 1$

ary is taken to be completely reflecting of both particles and waves. The injected particles have a high x–directed velocity component $u_{\mathrm{inj},x}$ and a random thermal velocity which corresponds to the upstream temperature T_1 (The indices 1 and 2 refer to the upstream and the downstream values respectively). The magnetic field at the upstream (left) boundary is fixed at $B_{z,1}$. The shock will then form at the right boundary and propagate to the left.

In order to simulate the shock for longer times without increasing the size of the box, we have developed a simple shock following algorithm. After the system has evolved for some time, the shock will on average be at rest in the simulation box. However all physical quantities in the simulation will be given in the downstream rest frame.

In the following we will use normalized quantities. The x–coordinate is normalized by the ion Larmor radius λ_{ci} which is calculated with the upstream velocity $u_{1,x}$ in the shock rest frame and magnetic field B_1. The velocity is normalized by the injection velocity of the upstream plasma $u_{\mathrm{inj},x}$, the magnetic field by the upstream magnetic field $B_{z,1}$ and the electric field by $u_{\mathrm{inj},x}B_{z,1}$.

Here we show the results of two simulations, with different plasma β. The first simulation with $\beta = 0.15$ corresponds to the shock simulated by Shimada and Hoshino (2000). The other run has a considerably higher value of $\beta = 1$. The other parameters in both simulation runs are chosen to be the same as in the Shimada and Hoshino case: the ratio of electron plasma to Larmor frequency $\omega_{pe}/\Omega_{ce} = 20$ and the ratio of ion to electron mass $M/m = 20$. The upstream perpendicular magnetic field, which was not specified by Shimada and Hoshino, is assumed to be $B_{z,1} = 10^{-7}$Tesla. This value is consistent with those expected in supernova remnants (eg Ellison and Reynolds (1991)).

The dimension of a grid cell is equal to the initial Debye length while the size of the simulation box is set to a few times the upstream ion Larmor radius ρ_{i1}. This results in a simulation box of 5000 grid cells for $\beta = 1$ and 15000 grid cells for $\beta = 0.15$. Initially each grid cell contains about 100 particles of each species. The calculation was carried out on 40 processors of a Cray T3E. The total CPU time was about 60 hours for the low β case and 30 hours for the high β case.

3 Results

The first simulation was carried out for $\beta = 0.15$ which corresponds to the parameter value investigated by Shimada and Hoshino (2000). In Figure 1 we show the ion and electron v_x vs. x phase space distributions after about $5/\omega_{ci}$ (where $\omega_{ci} = eB_1/m_i$ is the upstream ion cyclotron frequency) together with the perpendicular magnetic field B_z, and the parallel electric field E_x. At this time the shock is well separated from the wall and is kept close to the left boundary ($4\lambda_{ci}$) of the simulation area. (Note that the origin of Figure 1 does not coincide with the origin of the simulation box.)

In the simulations with $\beta = 0.15$ we reconstruct the results of Shimada and Hoshino (2000). The shock shows a complex structure, with a high fraction of the ions reflected at the shock, forming the upstream foot of the shock. The electron phase space distribution in Figure 1 exhibits electron phase space holes at those points where substructures in the ion phase space can be observed. These are associated with large peaks in the electric field.

In contrast the simulations with $\beta = 1$ show no small scale structure, see Figure 2. As in the low beta case a fraction of the ions $f(v)$ is reflected at the shock front and form the foot of the shock. While the phase space distribution in the region downstream of the shock still shows structure, there is no small scale structure in the foot region like that seen in Figure 1. The phase space distributions of ions and electrons in the foot show a high thermal spread compared to the low β case.

We now look at the temporal behavior of the shock. Figure 3 shows the perpendicular magnetic field as a function of position and time. We clearly see the non stationary behavior

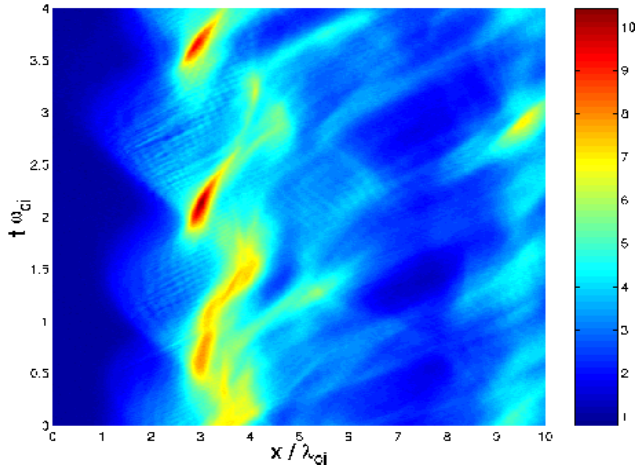

Fig. 3. The perpendicular magnetic field component B_z as a function of position and time for $\beta = 0.15$. The field is normalized to the upstream magnetic field.

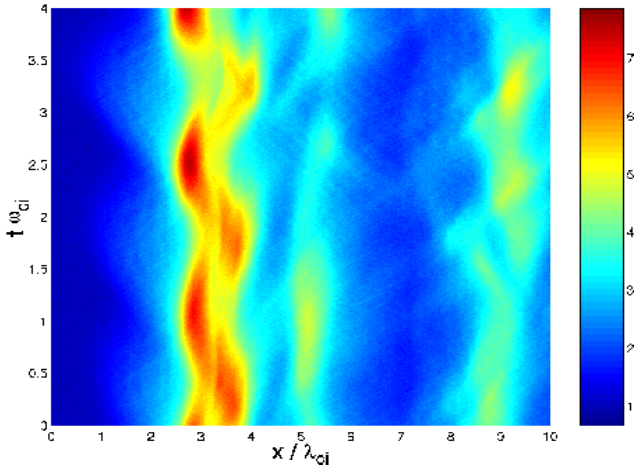

Fig. 4. The perpendicular magnetic field component B_z as a function of position and time for $\beta = 1$. The field is normalized to the upstream magnetic field.

of the shock front. The magnetic overshoot region, corresponding to the maximum in the magnetic field (red colour) moves back and forth in the shock in a more or less periodic fashion on the time-scale of the ion cyclotron period. The magnetic overshoot is repeatedly pushed back into the downstream region while a new maximum in B_z further upstream is created. At the same time the size of the foot of the shock increases and decreases. In the foot formation period starting at about $t\omega_{ci} = 2$ one can clearly see that — while the size of the foot is increasing — a wave with a phase velocity directed upstream travels into the foot. These waves have a wavelength of order the electron Larmor radius. As the shock progresses through a cycle the phase velocity of these waves decreases and reaches zero before increasing again. Shortly before the maximum extension of the foot, modes with a downstream directed phase velocity appear in the perpendicular magnetic field. These waves also have a wavelength comparable to the electron Larmor radius, but their phase velocity and hence their frequency is much larger. The last maximum of this second wave mode seems to be initializing the next magnetic overshoot. With this the foot almost dies down and a new cycle begins.

The $\beta = 1$ results (Fig. 4) do not show this involved time dependence. The magnetic overshoot region oscillates in the x–direction and the size of the foot region pulsates with the same time period, which is of the order of the ion cyclotron time. However no waves are observed in the foot region, and the shock shows no signs of reformation events.

4 Analysis

To quantify the differences in the foot of the shock for the two cases $\beta = 0.15$ and $\beta = 1$ we have taken a small region ($0.08 < x/\lambda_{ci} < 3.92$; $2.45 < t\omega_{ci} < 2.90$ for $\beta = 0.15$ and $0.97 < x/\lambda_{ci} < 2.21$; $1.13 < t\omega_{ci} < 2.28$ for $\beta = 1$) and that lies inside the foot region. The perpendicular magnetic field and the parallel electric field were sampled with 512×2048 grid points for $\beta = 0.15$ and 256×2048 grid points for $\beta = 1$ in the x and t direction. A two dimensional Fourier transform was applied after Hanning windowing to compensate for the non periodicity of the data.

The low β Fourier transformed fields $\hat{B}_z(k,\omega)$ and $\hat{E}_x(k,\omega)$ show very clear structure, see Figs 5 and 6. Two different modes can be observed in the perpendicular magnetic field. The first mode (at higher ω) shows a hyperbolic shape in ω–k–space which crosses the ω–axis at about 1.5 to $2\omega_{pe}$ (here the electron plasma frequency is calculated with the upstream undisturbed conditions). Assuming a density rise of a factor 3 in the foot as compared to the upstream plasma the plasma frequency would be $\sqrt{3}\omega_{pe} \approx 1.73\omega_{pe}$. Another clearly visible mode in the diagram intersects the origin with a constant negative slope. This mode corresponds to the low frequency waves that are observed in Figure 3 traveling back from the shock into the foot.

The electric field parallel to the flow (Fig.6) exhibits wide spectrum noise but with a maximum at the same negative phase velocity mode as observed in the perpendicular magnetic field. Moreover a clear cutoff with a hyperbolic shape that does not coincide with the mode observed in $\hat{B}_z$ can be seen.

The Fourier transforms of B_z and E_x for the case of $\beta = 1$ show the same modes, however at a much lower level than for the low β case.

5 Electron Acceleration

Finally we have determined the energy distribution of the electrons in the far downstream region. To this end we have calculated the absolute value of the velocity of every electron in the rightmost ion Larmor radius of the simulation and distributed them into 1000 velocity bins. To improve the statistics we have repeated this for every time-step over one ion

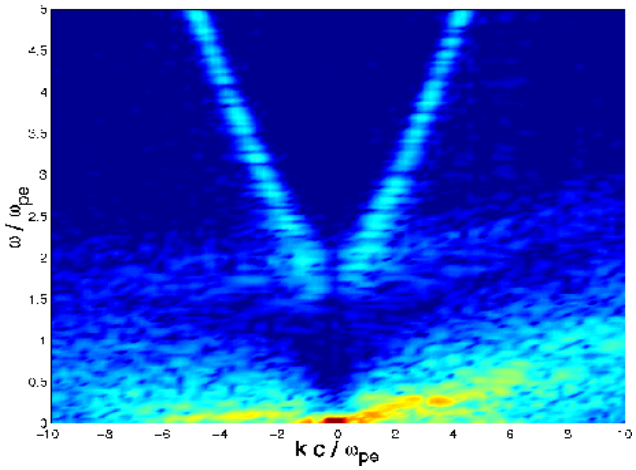

Fig. 5. The Fourier transform of the perpendicular magnetic field B_z in the foot of the shock for $\beta = 0.15$.

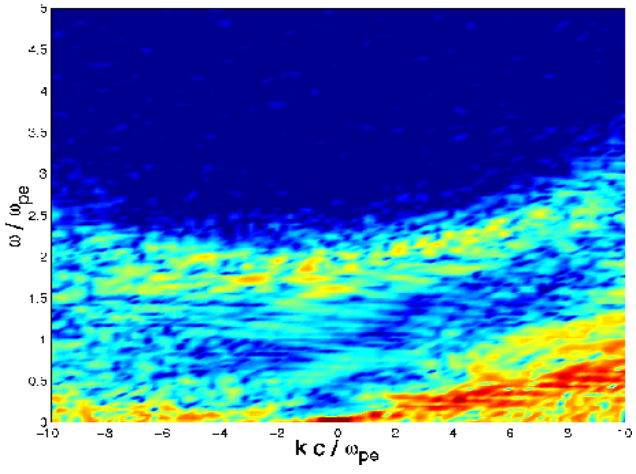

Fig. 6. The Fourier transform of the parallel electric field E_x in the foot of the shock for $\beta = 0.15$.

cyclotron period and integrated the results. The resulting energy distributions $f(E)$ for $\beta = 0.15$ and $\beta = 1$ are shown in Figure 7. The energy is normalized to the inflow kinetic energy of the electrons and in addition $\int_0^\infty f(E)\, dE = 1$.

The two energy distributions shown in Figure 7 demonstrate that the value of β has great influence on the thermalisation and acceleration of electrons in the shock. The distribution in the high β case is almost thermal. The temperature is calculated by regression to be $T_e = 3.08 \frac{mu_{\rm inj}^2}{2}$ which is also plotted in Figure 7. The energy distribution for the low β case on the contrary can be described by two temperatures. Up to about 20 times the injection energy the distribution follows a thermal distribution with $T_e = 2.90 \frac{mu_{\rm inj}^2}{2}$. Above 30 times the injection energy the distribution shows a high energy tail with a temperature of $T_e = 5.75 \frac{mu_{\rm inj}^2}{2}$. This suggests that the increased level of wave activity in the foot of the shock for the low β case is very efficient in accelerating the electrons.

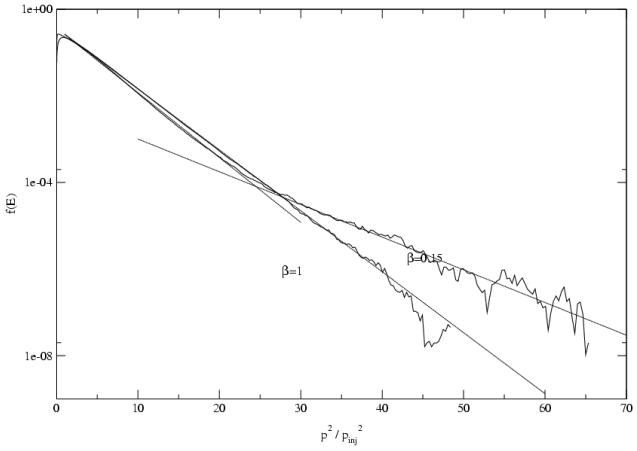

Fig. 7. The energy distribution of electrons for $\beta = 0.15$ and $\beta = 1$ averaged over the rightmost ion larmor radius of the simulation box and over one ion cyclotron period.

6 Conclusions

We have simulated a high Mach number magnetosonic shock of a supernova remnant for two different values of the kinetic to magnetic pressure ratio β. The two cases were found to exhibit different behaviour of the foot of the shock resulting in a difference in the electron acceleration. While the high β case yielded a purely thermal downstream electron distribution, the electron distribution of the low β case could best be modeled with two different temperature populations. This distribution had a very high temperature tail, thus the low β shock is much more efficient at accelerating electrons than the high β shock.

Acknowledgements. This work was supported in part by the Comission of the European Communities, TMR Astroplasmaphysics Network Contract ERB-CHRXCT980168. We are grateful to K. G. McClements for helpful comments.

References

Blandford R.D., Ostriker J.P., ApJ **221**, L29 (1978)
Cargill P.J., Papadopoulos K., ApJ **329**, L29 (1988)
Devine P., Ph.D. Thesis, University of Sussex, 1995
Dieckmann M. E. *et al.*, Astron. Astrophys. **356**, 377 (2000)
Drury L. O'C., McClements K. G., Dendy R. O., Chapman S. C., Dieckmann M. E., Ljung P., Ynnerman A., *Computational Studies of Cosmic Ray Electron Injection*, these proceedings
Ellison D. C., Reynolds S. P., ApJ **382**, 242 (1991)
Hockney R.W., Eastwood J.W., *Computer Simulations using Particles*, McGraw Hill, New York 1981
Koyama K., Petre R., Gotthelf E.V. *et al* Nat **378**, 255 (1995)
Levinson A., MNRAS **278**, 1018 (1997)
Papadopoulos K., Ap&SS **144**, 535 (1988)
Shimada N. and Hoshino M., Astrophys. J. **543**, L67 (2000)